Optimizing Energy Harvesting Parameters using Response Surface Methodology

P. Mane, K. Mossi, and C. Green

***Abstract*—Energy harvesting is a process in which energy which would otherwise be wasted is stored and then used to power a system. Due to their unique properties piezoelectric materials are ideal for energy harvesting applications. In this study a pre-stressed piezoelectric composite is pressure loaded dynamically to harvest energy. The objective of this study is to optimize relevant parameters that have an effect on the energy harvesting process using piezoelectric diaphragms. Parameters considered are temperature, pressure, resistance and frequency. Response surface methodology is used to develop models to identify optimal parameter ranges and also to predict power conversion capabilities for specific parameter levels. Power densities of approximately 24.27μW/mm^3 are measured at optimal conditions. The model identifies optimal temperature of 12°C and 240kPa for pressure which are in agreement with experimental results.**

***Index Terms*—energy harvesting, pre-stressed, piezoelectric composite, regression models, response surface methodology**

I. Introduction

ENERGY harvesting is a process in which energy which would otherwise be wasted is processed and stored for future use by an application. The use of harvested energy could extend the operational life of devices traditionally powered by batteries. This is particularly advantageous in systems with limited accessibility such as biomedical implants and structures with embedded micro and wireless sensors. It is feasible that such devices would have the ability to generate their own power from the ambient environment. This can either prolong the life of an existing battery or eliminate the battery. With advances in design and manufacturing as well as reduced power requirements, the use of energy harvesting methods have become practical and has gained significant popularity [1, 2].

There are several types of ambient energy which exist in nature that can be harvested. Heat, electricity, solar, and biomass are forms of energy that are stored differently, but can be converted from one form to the other. Photocells convert light to electricity, thermocouples convert heat to electricity, and magneto-electric generators convert mechanical energy to electricity. These are all power generators and are frequently used in electricity generation. Similar to magneto-electric generators, piezoelectric materials can also convert mechanical energy from vibrations to electrical energy.

Piezoelectric power generators can be advantageous for some systems over other conversion methods. Because of their simplicity, they can be made small enough to fit inside of micro electromechanical systems (MEMS) [3]. Another advantage is that lifetime of the system is extended if the applied force and external temperature are within the operational range of the piezoelectric material. The mechanical energy required for conversion can feasibly be obtained from the environment. Even with these advantages, until recently, piezoelectric generators have been neglected for power generation because of the small electrical output. But with advances in integrated circuit technology this is no longer an issue. Other problems with piezoelectric generators are application specific so that a common solution does not exist. Hence, power requirements are different to a variety of modules, thus suitable circuitry is required to adapt to various applications. In the current study, relevant factors are identified and a process through which these parameters can be optimized is outlined.

Piezoelectric materials are versatile because vibrations occur in most dynamic systems. These materials also have a wide dynamic range and low output noise. There are many piezoelectric materials from which to choose for designing a power conversion mechanism. Roundy et al. have shown that a power density of 70μW/cm^3 is quite feasible from a PZT bimorph beam mounted as a cantilever. Simulations by the same investigators show that an optimized design would be capable of 250μW/cm^3 from a vibration source with input vibrations of 2.5m/s^2 at 120Hz [3-5]. Erika et al. modeled and tested a Unimorph membrane consisting of PZT and brass encircled by an aluminum ring mounted on a mechanical shaker [6]. The excitation of the shaker was varied between 0-5g of acceleration. The electrical output of the membrane was connected to load resistors which varied from 100Ω to 1MΩ. It was found that a maximum power of 1.8mW was generated at an acceleration of 2g with a 56kΩ load resistance. Yoon, Washington, and Danak studied the charge generation properties of curved rectangular PZT Unimorph beams by optimizing geometric parameters such as length, width and thickness of the device [7]. A shoe insert which was used in a previous study to harvest energy while walking, was modeled using the piezoelectric constitutive equations and the shallow, thin shell theory. An equation was derived that expressed charge generation of the PZT beam in terms of applied force,

Manuscript received April 28, 2008.

P. Mane is with Virginia Commonwealth University, Richmond, VA, 23284 USA (phone: 804-827-5275; fax: 804-827-7030; e-mail: manepp@vcu.edu).

K. Mossi, is with Virginia Commonwealth University, Richmond, VA, 23284 USA (e-mail: manepp@vcu.edu).

C. Green was with Virginia Commonwealth University, Richmond, VA, 23284 USA, is now with Naval Surface Warfare Center, Dahlgren, VA, 22448 USA (e-mail: cwgreen@vcu.edu).

material properties and geometry. In a parametric study using the dimensions from nine samples, it was shown that geometry and material properties do affect charge production. Increasing the width, center height, and the thickness of the substrate produces increased charge generations. During this study, an experiment was conducted by dropping a 5lb weight on a sample and determining its charge production. Another experiment was conducted by determining the charge production of a sample while a 100lb human stepped on it.

An additional aspect of the energy harvesting process is signal conditioning, as the electrical charge generated by a piezoelectric generator is usually insufficient to power a commercial device. By using circuitry the generated signal is processed such that a usable voltage is obtained which can be applied to the device directly or used to charge a battery [8]. The type of circuitry used to harvest the energy from a piezoelectric transducer is determined by the desired output to the load which most often needs to be rectified, filtered, and regulated [9]. To that end, a piezoelectric transducer can be modeled as an AC source in parallel with a capacitor. To convert this signal into a useful one, an AC-DC converter is used to rectify the AC signal. The output from this converter is then sent to a DC-DC converter where it is regulated to the desired voltage. Roundy et al. explored the possibility of scavenging low level vibrations as a power source for wireless sensor nodes. In this study, the geometry of the piezoelectric device was optimized while the load resistance of the circuitry, which consisted of a series inductor with an active bridge, was varied. A piezoelectric generator was modeled as an AC source in series with a capacitor, and a resistance [3-5]. Other approaches include the use of piezoelectric composites. Sodano, Lloyd, and Inman for instance, compared the ability of a three different types of composites to convert mechanical strain into electrical energy by exciting them while attached to an aluminum beam. Their study concluded that impedance matching between the transducer and the circuit is critical when optimizing for power [10, 11].

Mossi et al. performed an investigation of parameters that affect actuation and energy harvesting on rectangular pre-stressed piezoelectric Unimorphs [12]. Parameters such as conductivity of the adhesive, composition, size, type and thickness of the layers, were investigated using fractional factorial experimental design techniques. Statistical analyses of all the results were performed to determine the significance of the parameters tested. The study concluded that circuitry must be coupled with device geometry to optimize its performance.

In this study the energy harvesting system is optimized using response surface models. Based on a literature review physical and environmental parameters of temperature (*T*), pressure (*P*), frequency (*f*) and circuitry parameters of and resistance (*R*) are used in the study. In a study by Mossi et al the stiffness of a piezoelectric composite was shown to be temperature dependent [13]. Changing composite stiffness affects the piezoelectric coefficients and in turn could affect the energy harvesting properties of the device. Also some of the possible applications where piezoelectrically harvested energy could be used operate in extreme environmental conditions making the effect of factors like temperature critical for implementation. Statistical methods are employed to explore the parameter. Using Response Surface Methodology modeling the point of inflection or the stationary point that optimizes power generation is calculated. The factor levels at the stationary point indicate the optimal parameter values.

II. EXPERIMENTAL SETUP

A. Piezoelectric Composite®

The devices used in this study are pre-stressed piezoelectric composites. They were chosen for their rugged construction and high performance when used as an actuator and a sensor [14]. The composite has an active PZT-5A layer sandwiched between a top and bottom layer of dissimilar metals bonded with a high temperature polyimide adhesive (SI) [14]. The sandwich is assembled and then heated to 325ºC under vacuum. During cooling, the different coefficients of thermal expansion of the dissimilar metals cause the curved shape that is unique to pre-stressed devices. The bottom SI layer between ceramic and steel contains conductive inclusions which have been shown to enhance energy harvesting properties [15]. The device used in this study is a circular diaphragm in which the top layer of metal is type 102 copper that has been perforated through chemical etching to change its stiffness. The bottom layer of metal is type 302 stainless steel. The piezoelectric layer was a soft PZT-5A ceramic with a material type of 3195HD manufactured by CTS Communications Components, Inc. The exact geometry is described in Table 1 and Fig. 1 shows a schematic of the device with its layer composition.

TABLE 1
DIAPHRAGM GEOMETRIC PARAMETERS

Thickness (total)	0.68mm (0.0295in)
Thickness (ceramic)	0.25mm (0.010in)
Diameter (total)	66.12mm (2.60in)
Diameter (ceramic)	61.72mm (2.44in)
Weight	14.5g (0.509oz)

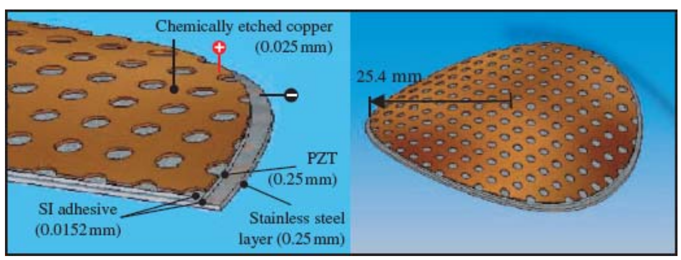

Fig. 1 A cutaway of a circular pre-stressed piezoelectric composite

B. Pressure and Temperature Setup

The diaphragm was dynamically pressure loaded using an air compressor such that the resultant vibrations produce a voltage. The device was clamped along its edges in a circular cavity which was pressurized using air on the copper side of the device while the steel side is left open to the ambient air. Fig. 2 a and b show a schematic of the energy harvesting cavity with connection for pressurization.

A block diagram of the complete experimental setup is shown in Fig. 3. Clean dry air (CDA) was sent to a model 42K75 regulator/filter combination manufactured by SpeedAire with a 0-827.4kPa (0 - 120psi) pressure gauge. The regulated pressures used during this study are 138kPa (20psi),

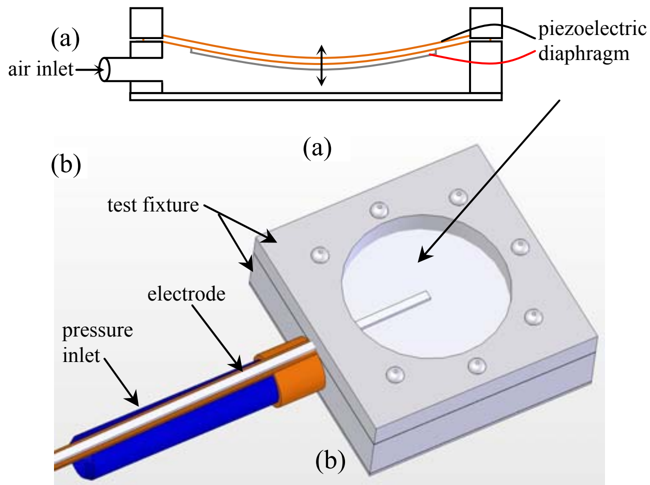

Fig. 2 Pressure cavity with diaphragm a) Cutaway schematic and (b) assembly

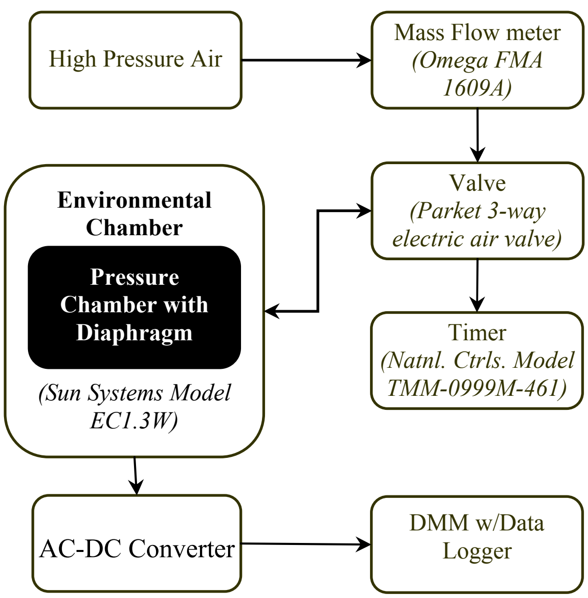

Fig. 3 Experimental Setup

206.85kPa (30psi), 275.8kPa (40psi), and 344.75kPa (50psi). During initial testing it was found that the limits of the flow meter were reached at a dynamic pressure of 50psi (344.75kPa) thus this value is set as the experimental limit. The air is then sent through an Omega FMA 1609A flow meter which measured mass and volumetric flow rate, temperature, and absolute pressure of the air entering the pressure chamber. A three-way electric air valve routes air into the pressurized cavity. Using an adjustable timer manufactured by National Controls Corporation model TMM-0999M-461, the valve is switched on and off at desired frequencies. The frequencies (2.5Hz, 3.25Hz, and 5Hz) used in this study were determined by the dynamic limitations of the 3-way valve. The pressure housing was enclosed in an environmental chamber from Sun Systems Model EC1.3W capable of heating up to 350ºC. While in the chamber, the diaphragm can be heated to desired temperatures.

C. Energy Harvesting Circuit

The passive rectifier circuit was chosen as the energy harvesting circuit because of its simplicity and lack of active components which consume power. A schematic of the circuit is shown in Fig. 4. The first stage of the circuit which is in parallel with the diaphragm is a RB114 Full Wave Bridge Rectifier. A Full Wave Bridge Rectifier converts AC to DC using a system of four diodes arranged such that the polarity in is the same as the polarity out. Each time a signal travels through the diode network; there is a voltage drop that depends on the characteristics of the diode. When attached to a load, marked at R in figure, the negative part of an input sine wave is removed and the frequency is increased by a factor of two. The output DC voltage deviates from a constant DC voltage by a parameter called a ripple voltage. When a capacitor is added, as represented by C in Fig. 2, ripples are smoothed and transients are filtered [16].

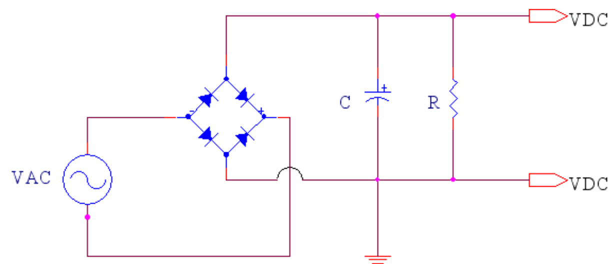

Fig. 4 Energy harvesting circuit

In the first set of experiments the peak to peak AC voltages are measured without using the energy harvesting circuit. The experiments are conducted at four pressures, 138kPa, 206.85kPa, 275.80kPa, 344.75kPa; three frequencies, 2.5Hz, 3.25Hz, 5Hz; and temperatures ranging from -60^{o}C to 100^{o}C at 10^{o}C intervals. The data is acquired using Tektronix TDS2024 oscilloscope and data acquisition software.

The second set of experiments was conducted using the energy harvesting AC-DC converter circuit. A standard 4.7µF capacitor is used while three loads of 470kΩ, 1MΩ and 2MΩ. The output DC voltage of the energy harvesting circuit was measured over a time interval to observe the charging and discharging behavior of the circuit. The DC measurement experiments are also conducted under the same physical conditions used in the first set of experiments using a DMM data logger device. The results from the experiments are described in the following sections. The data is also used in developing statistical models described in the next sections.

III. RESULTS

An experimental plan is developed according to the parameters tested using design of experiments theory. The ultimate goal of the experiments is optimization of harvested energy from a pre-stressed piezoelectric diaphragm. The diaphragm was mechanically actuated using air in a pressurized chamber and the electrical energy converted was measured. The optimizing parameters were temperature (*T*), pressure (*P*), frequency (*f*) and resistant (*R*).

A. Experimental Results

The AC voltages generated by the diaphragm oscillations are measured across the diaphragm without the use of a circuit. A typical AC waveform is shown in Fig. 5. The curve shown in Fig. 5 was measured at room temperature and 275.80kPa of dynamic pressure. Depending on temperature the magnitude of voltage either increases or decreases. For clarity the other tested temperatures have been omitted from the figure. Although not shown in the figure analysis of the AC data indicates that voltages are also dependent on applied pressure. To show the dependence of temperature and pressure on AC voltage generation, a typical contour plot of the AC voltage is shown in Fig. 6, for 5Hz frequency experiments. The high and low voltage regions are clearly visible in the figure. High voltages were measured at pressures between 250kPa to 300kPa and at higher pressures the voltage decreases. Thus, indicating that the optimal pressure is in this range. Similar temperature ranges are difficult to identify although two regions about 20°C and -30°C show high voltages. Further analysis of this temperature and pressure dependence was conducted using DC measurements.

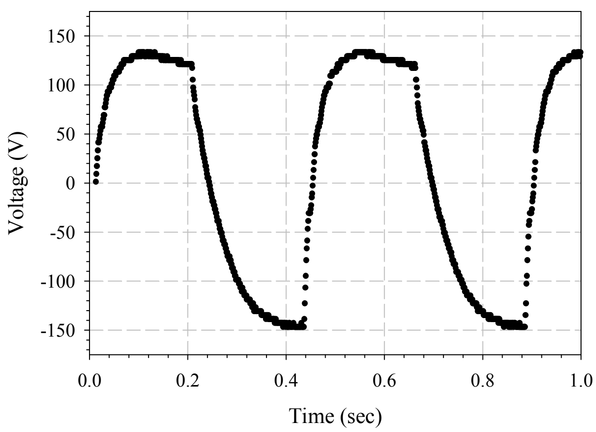

Fig. 5 Typical harvested AC voltage curve

The piezoelectric diaphragm was driven at three different frequencies. Fig. 7 shows the effect of frequency on the peak to peak AC voltage measured at 344.75kPa. As seen in Fig. 7, the three curves are almost identical indicating that frequency does not have any effect on the generated voltage. An ANOVA of the frequency levels was also conducted and the $F < F_{critical}$ condition was in agreement with the conclusions drawn from the graphs. Also the *p*-value of 0.5 was too large to consider frequency an important factor. These results are valid only at tested frequencies. At high excitation frequencies such as in the piezo resonance region this factor could become important. For the scope of this study, frequency is ruled out as a significant factor. Another observation from Fig. 7 is the peak in voltage seen at 20°C. This is seen at all frequencies and can help in identifying the optimal energy harvesting temperature.

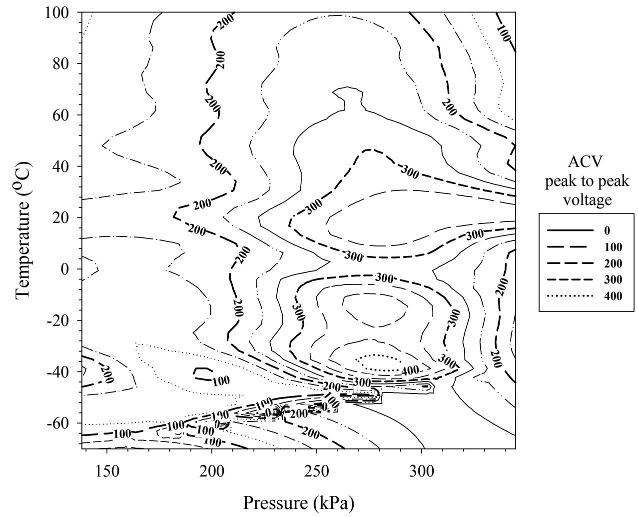

Fig. 6 Contour of AC voltage region

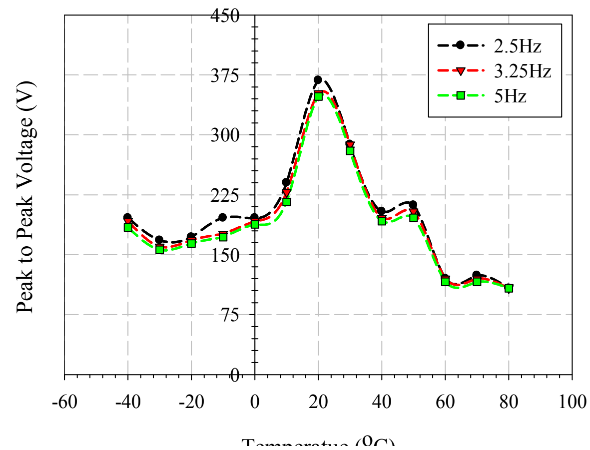

Fig. 7 Graph showing frequency effect

To utilize the harvested signal to power any device, the signal needs to be rectified to match the requirements of the device. Also most devices are powered with a DC voltage. To measure DC voltage an AC-DC converter circuit or energy harvesting circuit shown in Fig. 4, is added to the setup and the DC voltage is measured across a 4.7μF capacitor. In these experiments an additional factor of *R* is included in the study simulating a load in the circuit. By varying the resistance impedance matching is achieved with different devices. Impedance matching between the source and the device maximizes power transfer to the device making the system more efficient. Measurements are taken at different frequencies, resistances, temperatures and pressures. Typical DC voltage curves are shown in Fig. 8. The figure shows curves for 3.25Hz, 0°C and 344.75kPa measurements. The maximum voltage is measured at 2MΩ and the lowest at 470kΩ. Similar results are seen at other temperatures and pressures. This indicates that maximum voltage is transferred to the load at 2MΩ. Thus there is greater impedance matching between the source and the load at this resistance. When the harvested voltage is to be used to charge a battery or other storage device high impedance matching is required to ensure efficient use of the source. An ANOVA of the dc data also indicates that resistance is an important factor with a *p*-value of 0.00048 and the *F*-value of 89.43. It can be concluded that resistance is an important factor during energy harvesting and is dependent on the end application [10, 11]. However, a load of 2MΩ is not necessarily the optimal resistance for impedance matching. The optimal value can be obtained from response surface models described in the following sections.

Using the measured voltage and the available resistance values, instantaneous power is calculated through equation 1 shown below.

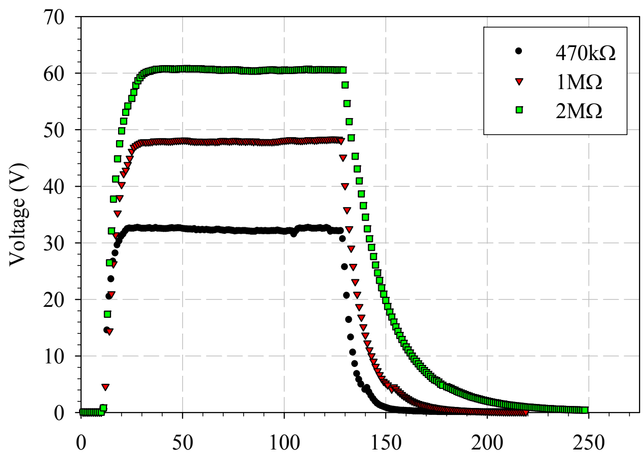

Fig. 8 Typical DC voltage curves

$$P = \frac{V^2}{R} \qquad \text{Equation 1}$$

Here V is the measured voltage in volts, R is the resistance in ohms and P is the power in Watts. The maximum calculated power was 18.44mW and using ceramic volume the maximum power density was found to be 24.27μW/mm^3. These values were obtained at 20^{o}C, 344.75kPa and 5Hz. A typical power graph is shown in Fig. 9. Calculating area under the power curve gives the energy harvested from the system as indicated by Equation 2.

$$E = \int_{t_i}^{t_2} P(t)dt \qquad \text{Equation 2}$$

P(t) is the instantaneous power and *E* is the total energy harvested by the device in Joules. The maximum total energy calculated was 3.05J at -60^{o}C, 206.85kPa and 2.5Hz. A typical power curve is shown in Fig. 9. The area of shaded portion of curve gives the energy as stated in equation 2. The results from this experiment were also compared with data published by Kim et al [17]. Kim et al. conducted experiments using a circular unimorph actuated with pressure. Although the magnitudes of pressure obtained in the current study are significantly higher the dimensions and construction of the piezoelectric diaphragms used in the two studies are different.

Visual analysis of the AC voltage data indicated that temperature and pressure were important factors which need to be studied further. Fig. 10 shows the effect of pressure on DC voltage measurements. The graph shows the peak DC voltages measured at several positive and negative temperatures at four increasing pressures. The temperatures follow a similar trend in which the voltage is maximum at 275kPa. The voltage increases up to this pressure and then decreases. This pressure can be identified as the optimal pressure for this energy harvesting setup.

As discussed previously the experimental measurements have identified trends in the energy harvesting process. In the following sections statistical methods are used to develop models which relate the variables under study. These relationships will further justify the experimental results. Furthermore such models can also be used in identifying optimal levels of the experiment indicating trends in the study.

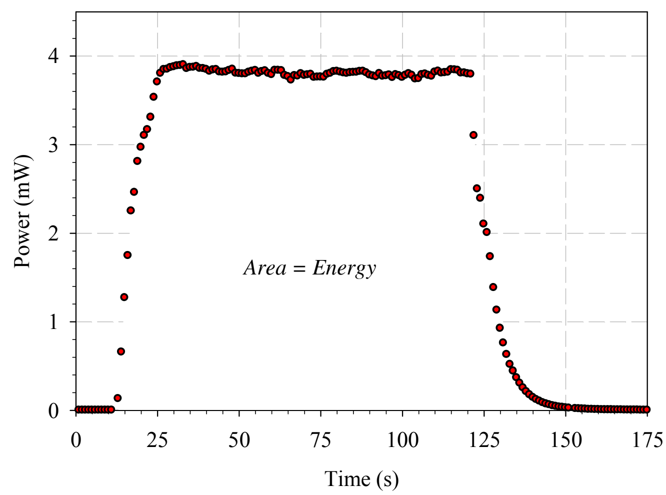

Fig. 9 A typical power curve

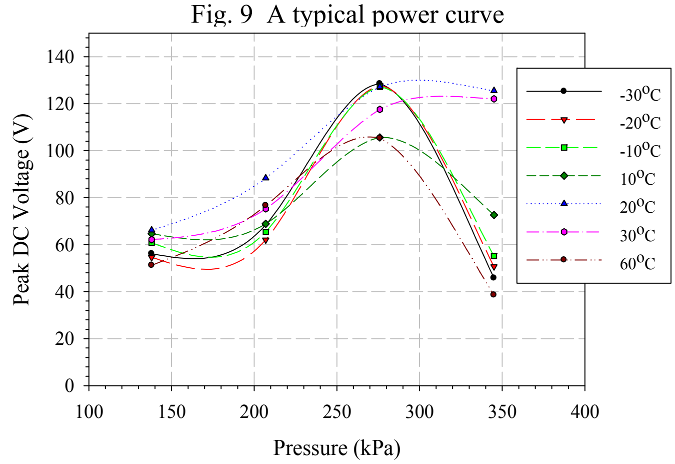

Fig. 10 Pressure effects on DC voltage

B. *Response Surface Model*

The Response Surface Methodology (RSM) is a collection of mathematical and statistical techniques useful for the modeling and analysis of problems. A response of interest is influenced by several variables and the objective of this methodology is to optimize this response. Given a response variable Y and n continuous factors, x_1, x_2,…, x_n, the main purpose of Response Surface Methodology (RSM), is to find the combination of factor levels to achieve the optimal response. In the current study the response variable (*Y*) is DC voltage and the factors or dependent variables to be modeled are resistant (*R*), pressure (*P*), temperature (*T*) and frequency (*f*).

The typical RSM procedure is described here as in many books such as Montgomery [18-20]. For computational convenience, the natural variables or factors are usually converted to coded or design variables, X_1, X_2, …, X_n, standardized so that the design center is at the point 0. In the current design there are three levels are designated as shown in Table 2, *-1*, *0*, *1*, in a confined region *R*.

TABLE 2
CODED FACTOR LEVELS

Levels	$R(\Omega)$	P(kPa)	T(°C)	f(Hz)
-1	470000	138	-40	2.5
0	1000000	275	20	3.25
1	2000000	350	80	5

The first step in RSM is to find a suitable approximation for the true functional relationship between *Y* and the set of independent variables as indicated by equation 3.

$$y = F(R, P, T, f) \qquad \text{Equation 3}$$

The relation is usually approximated by a polynomial of first or second degree in the confined region *R*. When a first order model does not yield a model the order is increased in an iterative process. A second order polynomial is used in particular when the interest is focused on the location of the stationary point or the point of inflection of the response function. The method of least squares is used to estimate the parameters in the approximating polynomials. With the aim of finding the maximum stationary point of the DC voltage response surface function, a second order polynomial model of the form shown in equation 4 is used in the analysis. Models are developed using computer softwares, *JMP IN 4* and *SigmaStat 3.1*.

$$y = \beta_0 + \sum_{i=1}^{n} \beta_i x_i + \sum_{i=1}^{n} \beta_{ii} x_i^2 + \sum_{i<j}\sum \beta_{ij} x_i x_j + \varepsilon \qquad \text{Equation 4}$$

$i = 1, 2, \ldots, n$ and $j = 1, 2, \ldots, n$

Here y is the response variable, x_1, x_2, …, x_n are the dependent factors, n is the number of factors, β_0 is the intercept term and β_i are the regression coefficients. ε is the random error which is assumed to be distributed as a normal distribution with zero mean and unknown variance. A regression analysis and model fit of the DC voltage data gives a second order polynomial model given in equation 5.The model fit has an R^2 value of 90%.

$$\begin{aligned} VDC = {} & 114.82 + 11.82R - 6.92P - 10.19T + 2.65f \\ & - 4.04RP - 3.51RT + 3.62PT - 1.04Rf + 2.60Pf + 0.27Tf \\ & - 9.73R^2 - 33.66P^2 - 20.84T^2 - 7.39f^2 \end{aligned}$$

Equation 5

As the fitted surface is an adequate approximation of the true response surface, analysis of the fitted surface is approximately equivalent to analysis of the actual system. The surface represented by the equation for VDC (response) shown in equation 5 is called the response surface. Response Surface plots and contour plots play a very important role in the study of the response surface. By generating these plots using computer software for response surface analysis, the shape of the surface can be characterized. Also, location of the optimum can be determined with reasonable precision. Figs. 11(a) and (b) show the response surface and the contour plot of response surface. The lines of constant response are drawn in the *T*, *P* plane. The dome shape of the response surface is result of the second order model fit. The optimal point is the peak of the dome; it can also be called the stationary point, saddle point or the maximum point.

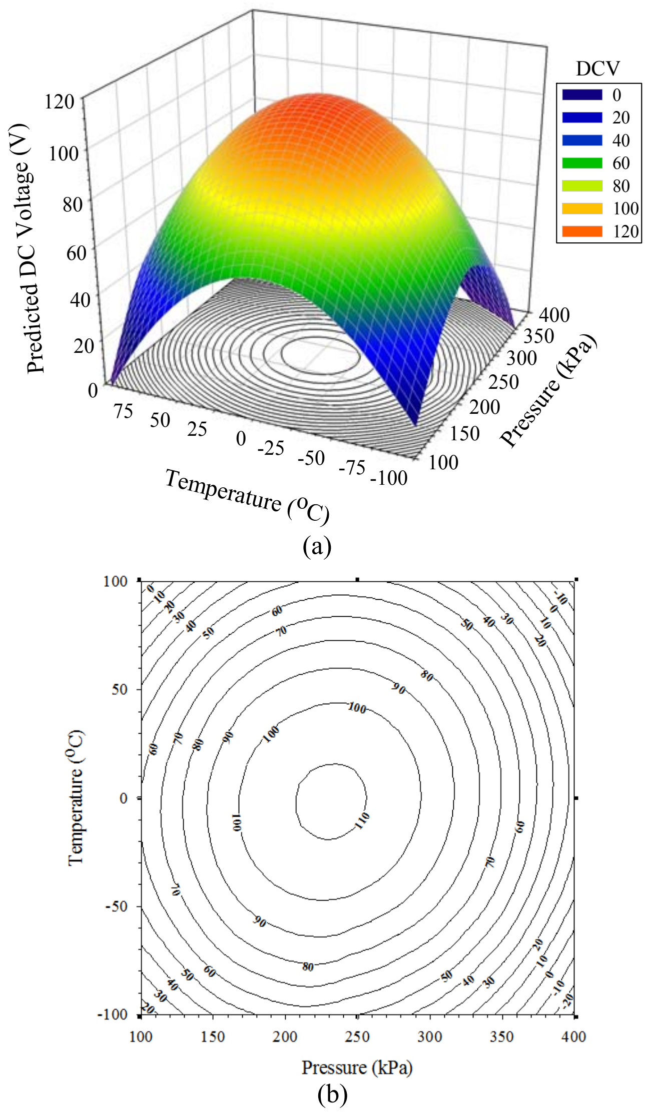

Fig. 11 (a) 3D Response surface showing the predicted DC voltage as a function of pressure (P) and temperature (T), (b) Contour plot of the response surface

1) Location of stationary point

A stationary point represents the point of maximum response, to find the levels of R, P, T, and f that optimize the predicted response. To obtain a mathematical solution for the location of the stationary point the fitted second order model is compactly written as shown in equation 6.

$$y = \beta_0 + x^T b + x^T Bx + \varepsilon \qquad \text{Equation 6}$$

Where x is a n x 1 vector of factor levels, b is a n x 1 vector of regression coefficients β_i and B is a n x n symmetric matrix of regression coefficients with ith diagonal element equal to β_{ii} and the (ij)th off-diagonal element equal to (1/2)β_{ij}. For the stationary point to exist the partial derivative $\delta y/\delta x$=0. Thus from the fitted model, the estimated stationary point is computed using equation 7 where x_s is a n x 1 matrix which gives the optimal levels for the factors.

$$x_s = -\frac{1}{2}B^{-1}b \qquad \text{Equation 7}$$

By substituting equation 7 into equation 6 the predicted response at the stationary point can be found as shown in equation 8.

$$y_s = \beta_0 + \frac{1}{2}x_s^T b \qquad \text{Equation 8}$$

Performing the analysis discussed previously results in a x_s matrix with coded and natural factor values as shown in Table 3. Experimental results from previous section indicate that the optimal pressure level is approximately 250kPa which is in agreement with the predicted optimal level in the statistical analysis. Similarly 20^{o}C was identified as the optimal temperature level in the experimental results. The model predicts the optimal temperature at approximately 12^{o}C.

A surface map was plotted using optimal resistance and frequency values of 1MΩ and 3.7Hz respectively. The surface as shown in Fig. 12 has similar results of peak voltage at 12^{o}C and 237.6kPa. Similarly voltages can be predicted for intermediate factor levels not tested in the experiments within the tested ranges.

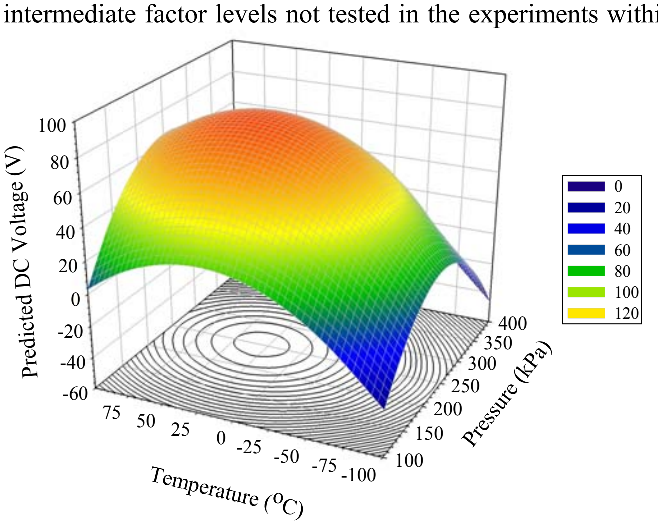

Fig. 12 Response Surface using optimal factor levels predicted in Table 3

Although PZT is a pyroelectric material, this effect is not involved in the study. For the pyroelectric effect to be significant the material has to be heated at a high heating rate [21]. Since the study has a very small heating and cooling rate (almost zero) the pyroelectric effect is zero and does not affect the outcome. The magnitudes of piezoelectric properties are dependent on piezoelectric coefficients of the material. The application of temperature and stress affects the coefficients and the functioning of the piezoelectric device. These stimuli are considered extrinsic contributions from the environment [22]. Under the application of a periodic stress, a near instantaneous charge is generated due to 180^{o} domain changes and some 90^{o} domain changes thus increasing the extrinsic contribution. As studied by Mukherjee et al. these effects are more prominent on soft ceramics such as PZT 5A due to more domain mobility. In another study it was shown that the response of a piezoelectric material to the application of stress is a non linear function of stress, time and temperature [23]. Thus there is a combined coupling effect which is also indicated in the regression model of equation 5. Along with having individual effects of the outcome each factor also affects the outcome coupled with the other factors. The piezoelectric response can also be affected by multiple heating [24]. In the current study the device is heated and cooled on several occasions without any time constant. These conditions could help in understanding the median values predicted by the regression models as the optimal conditions of the system. In a practical environment the conditions that the system will operate in will not be as varying as used in the current study. This study demonstrates that pre-stressed piezoelectric composites can be efficiently used to power devices and the efficiency is dependent on the operating conditions.

TABLE 3
OPTIMAL FACTOR LEVELS

Factors	Coded variables	Natural variables
R	0.692	1MΩ
P	-0.158	237.6kPa
T	-0.132	12^{o}C
f	0.097	3.7Hz

IV. Conclusion

A pre-stressed piezoelectric diaphragm was dynamically pressure loaded to harvest energy. Parameters involved in the energy harvesting process such as temperature, pressure, resistance and frequency are optimized using statistical techniques. Response surface methodology is used to develop models to identify optimal parameter ranges and also to predict power generation for specific parameter levels. The model predicted optimal levels of 12^{o}C, 237kPa, 1MΩ and 3.7Hz. These levels were in agreement with the experimental results. Maximum power densities of approximately 24.27μW/mm^3 are measured at optimal conditions. The results can be explained by studying the combined effect the factors have on the piezoelectric response of the material.

Piezoelectric coefficients are affected by stress and temperature and repeated heating and cooling cycles further introduce thermal hysteresis effects into the system.

The study demonstrates that pre-stressed piezoelectric composites can be used to power devices and response surface methodology can be utilized to optimize a system efficiently. In future studies the harvested energy can be collected in storage mediums to power small devices. As piezoelectric energy harvesting is operating conditions dependent using a storage medium could act as an interface between different applications.

ACKNOWLEDGMENT

The authors would like to thank Mathew Richeson and Alex Lichtenfels for all their assistance in the data collection process.

REFERENCES

[1] A. Chandrakasan, Goodman, R.J., Rabiner, W., "Trends in low power digital signal processing," presented at IEEE International Symposium on Circuits and Systems, 1998.
[2] W. R. Davis, Zhang, N., Camera, K., Markovic, D., Smilkstein, T., Ammer, M.J., Yeo, E., Augsburger, S., Nikolic, B., Brodersen, R.W., "A design environment for high-throughput low-power dedicated signal processing systems," *IEEE Journal of Solid-State Circuits*, vol. 37, pp. 420-431, 2002.
[3] S. Roundy, Wright, P.K., Rabaey, J., *Energy scavenging for wireless sensor networks : with special focus on vibrations*. Boston, MA: Kluwer Academic Publishers, 2004.
[4] S. Roundy, Wright, P.K., Rabaey, J., "A study of low level vibrations as a power source for wireless sensor nodes," *Computer Communications*, vol. 26, pp. 1131-1144, 2003.
[5] S. Roundy, "Energy Scavenging for Wireless Sensor Nodes with a Focus on Vibration to Electricity Conversion," in *Mechanical Engineering*. Berkley: University of California Berkley, 2003.
[6] M. Ericka, Vasic, D., Costa, F., Poulin, G., Tliba, S., "Energy harvesting from vibration using a piezoelectric membrane," *Journal de Physique IV France*, vol. 128, pp. 187-193, 2005.
[7] H. S. Yoon, Washington, G., Danak, A., "Modeling, Optimization, and Design of Efficient Initially Curved Piezoceramic Unimorphs for Energy Harvesting Applications," *Journal of Intelligent Material Systems and Structures*, vol. 16, pp. 877-888, 2005.
[8] N. Elvin, Elvin, A, Choi D.H., "A self-powered damage detection sensor," *The Journal of Strain Analysis for Engineering Design*, vol. 38, pp. 115-124, 2003.
[9] C. H. Park, "On the Circuit Model of Piezoceramics," *Journal of Intelligent Material Systems and Structures*, vol. 12, pp. 515-522, 2001.
[10] H. A. Sodano, Park, G., Leo, D.J., Inman, D.J., "Use of piezoelectric energy harvesting devices for charging batteries," presented at SPIE Smart Structures and Materials, San Diego, CA, 2003.
[11] H. A. Sodano, Lloyd, J., Inman, D.J., "An experimental comparison between several active composite actuators for power generation," *Smart Materials and Structures*, vol. 15, pp. 1211-1216, 2006.
[12] K. Mossi, Green, C., Ounaies, Z., Hughes, E., "Harvesting Energy Using a Thin Unimorph Prestressed Bender: Geometrical Effects," *Journal of Intelligent Material Systems and Structures*, vol. 16, pp. 249-261, 2005.
[13] K. Mossi, Bryant, R., and Mane, P., "Piezoelectric composites as bender actuators," *Integrated Ferroelectrics*, vol. 71, pp. 221–232, 2005.
[14] K. M. Mossi, Selby, G.V., Bryant, R.G., "Thin-layer composite unimorph ferroelectric driver and sensor properties," *Materials Letters*, vol. 35, pp. 39-49, 1998.
[15] C. W. Green, "Low Frequency Energy Harvesting Using Clamped Pre-Stressed Unimorph Diaphragms," in *Mechanical Engineering*. Richmond: Virginia Commonwealth University, 2006, pp. 132.
[16] P. Horowitz, Hill, W., *The Art of Electronics*. Cambridge, UK: Cambridge University Press, 1989.
[17] S. Kim, Clark, W.W., Qing-Ming, W., "Piezoelectric energy harvesting with a clamped circular plate: experimental study," *Journal of Intelligent Material Systems and Structures*, vol. 16, pp. 855-863, 2005.
[18] D. Montgomery, *Design and Analysis of Experiments*, Sixth ed. Hobokrn, NJ: John Wiley & Sons, Inc., 2005.
[19] G. E. Box, Draper, N.R., *Empirical Model Building and Response Surfaces*. New York: John Wiley & Sons, Inc., 1987.
[20] G. E. Box, Wilson, K.B., "On the experimental attainment of optimum conditions," *Journal of the Royal Statistical Society: Series B (Statistical Methodology)*, vol. 13, pp. 1-45, 1951.
[21] R. W. Whatmore, "Pyroelectric devices and materials," *Reports on Progress in Physics*, vol. 49, pp. 1335-1386, 1986.
[22] B. K. Mukherjee, Ren, W., Liu, S-F, Masys, A.J., Yang, G., "Non-Linear Properties of Piezoelectric Ceramics," presented at SPIE Smart Structures and Materials, San Diego, CA, 2001.
[23] S. Sherrit, Stimpson, R.B., Weiderick, H.D., Mukherjee, B.K., "Stress and temperature dependence of the direct piezoelectric charge coefficient in lead zirconate titanate ceramics," presented at SPIE Smart Structures and Materials, San Diego, CA, 1996.
[24] S. Sherrit, Yang, G., Wiederick, H.D., Mukherjee, B.K., "Temperature Dependence of the Dielectric, Elastic and Piezoelectric
Material Constants of Lead Zirconate Titanate Ceramics," presented at Smart Material, Structures and Systems, Bangalore, India, 1999.